



## Novel quinoxaline derivatives for in vivo imaging of $\beta$ -amyloid plaques in the brain

Mengchao Cui <sup>a,b</sup>, Masahiro Ono <sup>a,\*</sup>, Hiroyuki Kimura <sup>a</sup>, Boli Liu <sup>b</sup>, Hideo Saji <sup>a,\*</sup>

<sup>a</sup> Graduate School of Pharmaceutical Sciences, Kyoto University, 46-29 Yoshida Shimoadachi-cho, Sakyo-ku, Kyoto 606-8501, Japan

<sup>b</sup> Key Laboratory of Radiopharmaceuticals, Ministry of Education, College of Chemistry, Beijing Normal University, Beijing 100875, PR China

### ARTICLE INFO

#### Article history:

Received 17 March 2011

Revised 20 May 2011

Accepted 23 May 2011

Available online 27 May 2011

#### Keywords:

Alzheimer's disease

$\beta$ -Amyloid

Imaging agent

Binding assay

Autoradiography

### ABSTRACT

In a search for new probes to detect  $\beta$ -amyloid plaques in the brain of patients with Alzheimer's disease (AD), we have synthesized and evaluated a series of quinoxaline derivatives containing a '6+6' ring system. These quinoxaline derivatives showed excellent affinity for  $A\beta_{1-42}$  aggregates with  $K_i$  values ranging from 2.6 to 10.7 nM. Autoradiography with sections of brain tissue from an animal model of AD mice (APP/PS1) and AD patients revealed that [<sup>125</sup>I]5 labeled  $\beta$ -amyloid plaques specifically. In biodistribution experiments using normal mice, [<sup>125</sup>I]5 displayed high uptake (6.03% ID/g at 2 min) into and a moderately fast washout from the brain. Although additional refinements are needed to decrease the lipophilicity and improve the washout rate, the quinoxaline scaffold may be useful as a backbone structure to develop novel  $\beta$ -amyloid imaging agents.

© 2011 Elsevier Ltd. All rights reserved.

Alzheimer's disease (AD) is the most common form of dementia in older people, and is estimated to account for 50% to 70% of dementia cases. Senile plaques containing  $\beta$ -amyloid ( $A\beta$ ) aggregates and neurofibrillary tangles composed of highly phosphorylated tau protein are the two key pathological findings in postmortem AD brains.<sup>1,2</sup> The precise molecular mechanisms leading to the development of this disease are not fully understood, however, the amyloid cascade hypothesis is the most accepted explanation for the pathogenesis of AD.<sup>3</sup>

With modern functional neuroimaging techniques such as positron emission tomography (PET) and single photon emission tomography (SPECT), radio-labeled probes that specifically target  $A\beta$  plaques may aid in the diagnosis and monitoring of AD in living subjects. Thus, many efforts have focused on developing radiotracers or agents that allow  $A\beta$  imaging in vivo. An uncharged Thioflavin T (ThT) analogue, [<sup>11</sup>C]PIB (2-(4'-[<sup>11</sup>C]methylaminophenyl)-6-hydroxybenzothiazole), which is highly efficient both in crossing the blood-brain barrier (BBB) and in selective binding to  $A\beta$  plaques, is the most widely used amyloid marker with PET for amyloid imaging.<sup>4,5</sup> Recently, a close analogue of PIB, [<sup>11</sup>C]AZD2184 ([<sup>11</sup>C]-2-[6-(methylamino)pyridin-3-yl]-1,3-benzothiazol-6-ol), with a high affinity for  $A\beta$  fibrils in vitro was reported. Preliminary PET studies indicated that this probe displayed fast kinetics and an excellent contrast for  $A\beta$  plaques in the brain of AD patients.<sup>6,7</sup>

Compared with <sup>11</sup>C ( $t_{1/2}$ : 20 min), <sup>18</sup>F with a longer half-life ( $t_{1/2}$ : 110 min) would be more useful for routine clinical use. In fact, a <sup>18</sup>F-labeled PIB analogue, [<sup>18</sup>F]GE-067 ([<sup>18</sup>F]-2-(3-fluoro-4-(methylamino)phenyl)benzo[d]thiazol-6-ol)<sup>8</sup>, and two stilbene derivatives with fluorinated polyethylene glycol (PEG) units, [<sup>18</sup>F]BAY94-9172 ([<sup>18</sup>F]-4-(N-methylamino)-4'-(2-(2-(2-fluoroethoxy)ethoxy)ethoxy)-stilbene)<sup>9</sup> and [<sup>18</sup>F]AV-45 ([<sup>18</sup>F]-E)-4-(2-(6-(2-(2-(2-fluoroethoxy)ethoxy)ethoxy)pyridin-3-yl)vinyl)-N-methylaniline)<sup>10</sup>, are currently under phase II or phase III clinical trials. However, since the failure of [<sup>123</sup>I]IMPY ([<sup>123</sup>I]-6-iodo-2-(4-dimethylamino)phenyl-imidazo[1,2]pyridine) in clinical trials, there has been no report of any  $A\beta$  imaging agents for SPECT moving into clinical testing.<sup>11–13</sup>

Most of these  $A\beta$  probes were derived from the basic structure of thioflavin-T, which consists of a six-membered ring fused to a

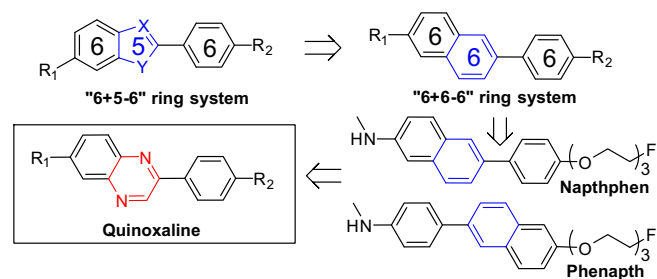
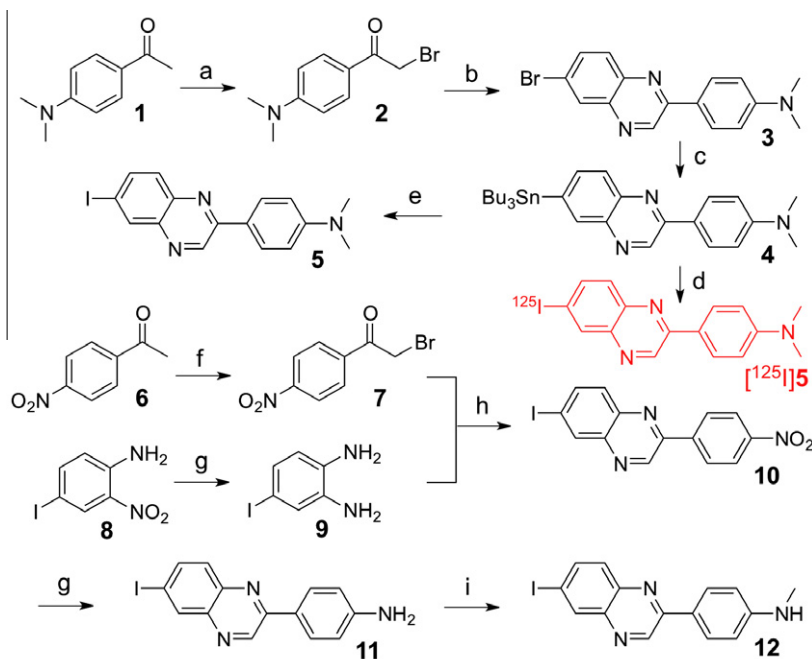


Figure 1. Design strategy for the quinoxaline derivatives as probes for  $A\beta$  plaques.

\* Corresponding authors. Tel.: +81 75 753 4608; fax: +81 75 753 4568 (M.O.); tel.: +81 75 753 4556; fax: +81 75 753 4568 (H.S.).

E-mail addresses: ono@pharm.kyoto-u.ac.jp (M. Ono), hsaji@pharm.kyoto-u.ac.jp (H. Saji).



**Scheme 1.** Reagents and conditions: (a) 1: conc.  $\text{H}_2\text{SO}_4$ ,  $\text{Br}_2$ ,  $0^\circ\text{C}$  to rt 2: ethyl phosphite,  $\text{Et}_3\text{N}$ , THF,  $0^\circ\text{C}$  to rt; (b) 4-bromobenzene-1,2-diamine, DMSO, rt; (c)  $(\text{Bu}_3\text{Sn})_2$ ,  $(\text{PPh}_3)_4\text{Pd}$ , dioxane,  $\text{Et}_3\text{N}$ , reflux; (d)  $[^{125}\text{I}]\text{NaI}$ ,  $\text{HCl}$  (1 M),  $\text{H}_2\text{O}_2$  (3%), rt; (e)  $\text{I}_2$ ,  $\text{CHCl}_3$ , rt; (f)  $\text{Br}_2$ ,  $\text{Et}_2\text{O}$ ,  $0^\circ\text{C}$  to rt; (g)  $\text{SnCl}_2$ ,  $\text{EtOH}$ , conc.  $\text{HCl}$ , reflux; (h) DMSO, rt; (i) acetone,  $\text{CH}_3\text{I}$ ,  $\text{K}_2\text{CO}_3$ .

five-membered heterocyclic ring together with another conjugated six-membered ring, creating a '6+5–6' ring system (Fig. 1). In an attempt to further develop novel ligands for the imaging of amyloid plaques through enlargement of the five-membered ring, Zhang et al. reported two fluoro-pegylated phenanthro or naphthphen derivatives as PET probes which contain a '6+6–6' ring system.<sup>14</sup> However, the naphthalene ring is highly lipophilic which may cause high non-specific binding. To reduce the lipophilicity, we have selected quinoxaline instead of the naphthalene ring. Herein, we report the synthesis and biological evaluation of quinoxaline derivatives as potential  $\text{A}\beta$  imaging agents.

The synthesis of quinoxaline derivatives is described in Scheme 1, starting from  $\alpha$ -bromoacetophenone and substituted

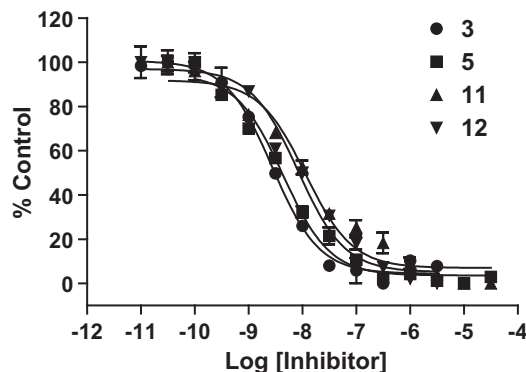


**Figure 3.** Inhibition curves for the binding of  $[^{125}\text{I}]\text{IMPY}$  to  $\text{A}\beta_{1-42}$  aggregates.

$o$ -phenylenediamines. The intermediates  $\alpha$ -bromoacetophenone (2 and 7) and 4-iodobenzene-1,2-diamine (9) were prepared first based on procedures reported previously.<sup>15</sup> In the presence of DMSO, the quinoxaline backbone was formed by an one-pot tandem oxidative condensation procedure in moderate yields (3: 36.7%, 10: 49.1%). Two isomeric products were obtained depending on the course of cyclization, the corresponding 2-aryl-6-substituted quinoxalines (3 and 10) as major products and the 2-aryl-7-substituted quinoxalines as minor products. Furthermore, the crystal structure of 3 was determined by X-ray crystallography (see Supplementary data). The free amino derivative 11 was achieved by reducing a nitro group to an amino group with  $\text{SnCl}_2$  in ethanol under reflux condition (87.0%). Conversion of 11 to the *N*-methylamino derivative 12 was achieved by methylation with  $\text{CH}_3\text{I}$  under alkaline conditions. The desired tributyltin precursor 4 was prepared by  $\text{Pd}(\text{PPh}_3)_4$ -catalyzed *trans*-stannylation from the bromide compound 3 (31.5%). The subsequent iodostannylation reaction afforded the iodinated target 5 (21.8%).

The desired radioiodinated ligand  $[^{125}\text{I}]\text{5}$  was successfully prepared from the corresponding tributyltin precursors through

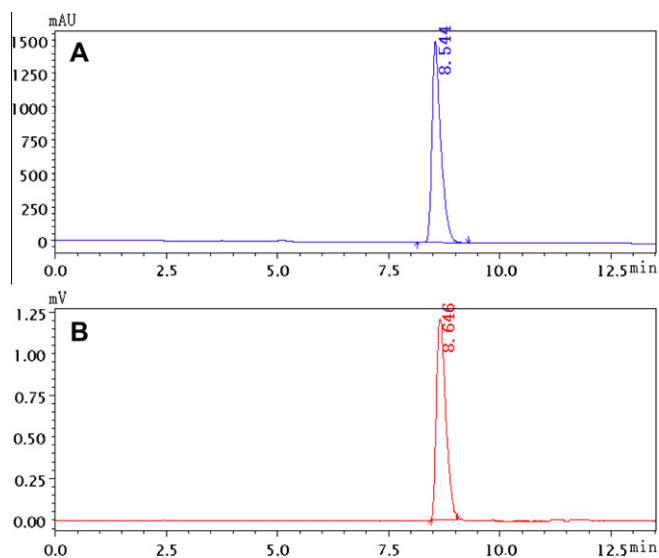


**Figure 2.** HPLC profiles of 5 (A) and  $[^{125}\text{I}]\text{5}$  (B). HPLC conditions: Cosmosil C18 column (Nakalai Tesque,  $5\text{C}_{18}\text{-AR-II}$ ,  $4.6\text{ mm} \times 150\text{ mm}$ ),  $\text{CH}_3\text{CN}/\text{H}_2\text{O} = 90/10$ ,  $1\text{ mL}/\text{min}$ , UV, 254 nm,  $5t_{\text{R}}$  (UV) = 8.54 min,  $[^{125}\text{I}]\text{5}t_{\text{R}}$  (RI) = 8.65 min.

**Table 1**  
Inhibition constants ( $K_i$ , nM) for the binding of [ $^{125}$ I]IMPY to  $A\beta_{1-42}$  aggregates.

Compound	R <sub>1</sub>	R <sub>2</sub>	$K_i$ (nM) <sup>a</sup>
<b>3</b>	Br	N(CH <sub>3</sub> ) <sub>2</sub>	2.6 ± 0.2
<b>5</b>	I	N(CH <sub>3</sub> ) <sub>2</sub>	4.1 ± 0.7
<b>11</b>	I	NH <sub>2</sub>	10.7 ± 1.1
<b>12</b>	I	NHCH <sub>3</sub>	7.7 ± 1.4
IMPY	—	—	10.5 ± 1.0

<sup>a</sup> Values are the mean for three independent experiments.

standard iododestannylation reactions, using sodium [ $^{125}$ I]iodide, hydrogen peroxide, and hydrochloric acid (Scheme 1). The overall radiochemical yield for [ $^{125}$ I]**5** was 62.3%. The radiochemical identity of the  $^{125}$ I-labeled ligands was confirmed by co-injection with nonradioactive compounds from HPLC profiles (Fig. 2). The purified ligands all had a radiochemical purity greater than 98% and high specific activity (no carrier added, approx. 81.4 TBq/mmol).

The affinity ( $K_i$ , nM) of the quinoxaline compounds was evaluated based on inhibition of the binding of [ $^{125}$ I]IMPY to aggregates of  $A\beta_{1-42}$  fibers in solution (Fig. 3). The results are presented in Table 1. All of the compounds showed excellent affinity for  $A\beta$

aggregates ( $K_i \leq 10$  nM). The results indicated that these quinoxaline derivatives bind to the same site as [ $^{125}$ I]IMPY. From the  $K_i$  values listed in Table 1, it is clear that the tertiary *N,N*-dimethylamino analogues **3** and **5** have higher affinity ( $K_i = 2.6$  and 4.1 nM, respectively) than the secondary *N*-methylamino analogue **12** ( $K_i = 7.7$  nM), while the corresponding primary amino analogue **11** showed moderate affinity ( $K_i = 10.7$  nM), which is consistent with previous data on primary, secondary, and tertiary amino ligands.<sup>16</sup> The  $K_i$  values of these quinoxaline derivatives are similar to that of phenanthroline or naphthalene derivatives ( $K_i = 1.6$  nM and 3.0 nM) reported previously.<sup>14</sup> Due to the encouraging binding data for these quinoxaline compounds, the tertiary *N,N*-dimethylamino analogue (**5**) was selected for radiolabeling and further biological evaluation.

To confirm the specific binding of **5** to  $A\beta$  plaques, the fluorescent staining of sections of brain tissue from an animal model of AD (C57BL6, APP/PS1 mouse, 12 months) was performed. As shown in Figs. 4, 5 clearly labeled  $A\beta$  plaques with low background levels (Fig. 4A), the labeling pattern consistent with that obtained on staining with thioflavin-S in adjacent sections (Fig. 4B).

Next, in vitro autoradiography was carried out in brain sections of AD patients and double transgenic mice using the radioiodinated

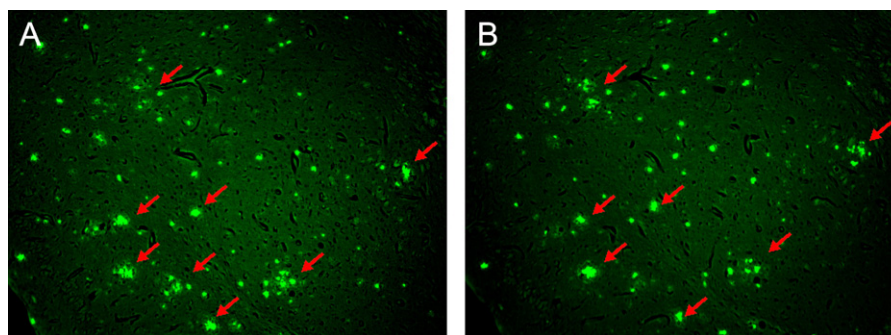


**Figure 4.** Fluorescence staining of **5** (A) in a section of brain tissue from a Tg model mouse (C57BL6, APP/PS1, 12 months old, male) with a filter set for GFP. The presence of plaques was confirmed by staining of the adjacent section with thioflavin S (B).

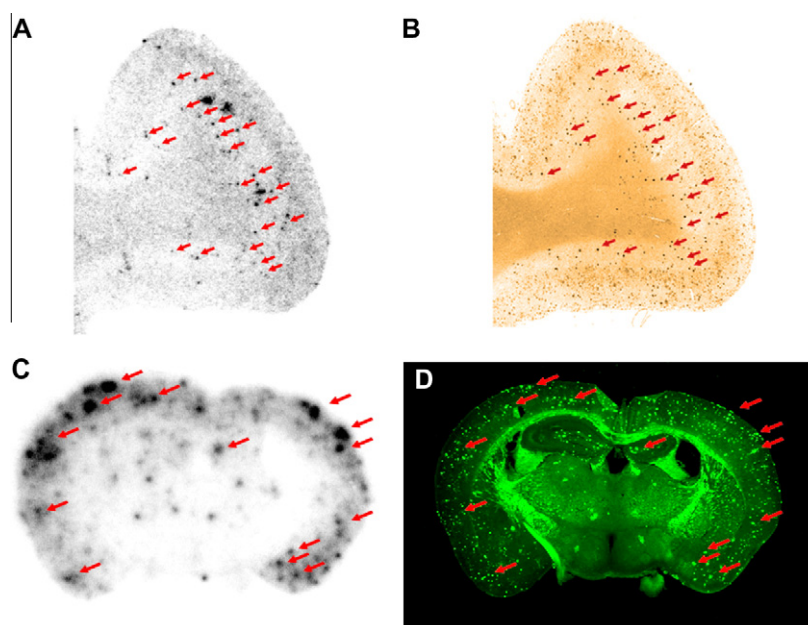


**Figure 5.** Autoradiography of [ $^{125}$ I]**5** in vitro in brain sections of an AD patient (A) and Tg mouse (C57BL6, APP/PS1, 12 months old, male) (C). The presence and distribution of plaques in the sections were confirmed with immunohistochemical staining using a monoclonal  $A\beta$  antibody (B) and thioflavin-S (D). Arrows show the correspondence to  $A\beta$  plaques.

**Table 2**  
Biodistribution in normal ddy mice after iv injection of [<sup>125</sup>I]5<sup>a</sup> and the lipophilicity (log *D*) of the ligand

[ <sup>125</sup> I]5 Log <i>D</i> = 4.02 ± 0.12				
Organ	2 min	30 min	60 min	120 min
Blood	4.71 ± 1.04	2.88 ± 0.62	2.98 ± 1.04	1.88 ± 0.55
Brain	6.03 ± 0.99	5.21 ± 1.16	2.91 ± 1.18	1.12 ± 0.31
Heart	14.91 ± 2.11	2.53 ± 0.77	2.17 ± 0.69	1.22 ± 0.29
Liver	30.49 ± 7.74	15.73 ± 3.76	12.50 ± 5.00	7.53 ± 2.51
Spleen	5.69 ± 1.79	2.82 ± 0.76	2.22 ± 0.86	1.17 ± 0.23
Lung	14.53 ± 5.53	3.99 ± 1.08	3.53 ± 1.27	1.95 ± 0.42
Kidney	19.67 ± 4.99	8.76 ± 2.72	6.68 ± 2.53	3.96 ± 0.96
Stomach <sup>b</sup>	2.06 ± 0.39	3.28 ± 0.72	5.39 ± 1.66	8.62 ± 2.40
Intestine	3.43 ± 0.83	18.62 ± 12.17	22.50 ± 9.17	16.93 ± 5.92

<sup>a</sup> Expressed as % injected dose per gram. Average for five mice ± standard deviation.

<sup>b</sup> Expressed as % injected dose per organ.

ligand [<sup>125</sup>I]5. As shown in Figure 5A, specific labeling of plaques was observed in AD brains. Immunohistochemical staining confirmed the presence of plaques in these sections (Fig. 5B). As expected, [<sup>125</sup>I]5 also labeled Aβ plaques in the brain sections of transgenic mice, with numerous fluorescent spots in the cortex region, and minimal background noise (Fig. 5C). The distribution of Aβ plaques was consistent with the results of autoradiography with thioflavin-S (Fig. 5D).

Although two nitrogen atoms were introduced into the aromatic system of the quinoxaline structure, a high log *D* value (4.02) for [<sup>125</sup>I]5 was obtained under the experimental conditions, a reflection of the lipophilic properties of the radioiodinated ligand. Nonetheless, biodistribution experiments in normal mice (Table 2) clearly indicated that [<sup>125</sup>I]5 readily penetrated the intact BBB showing excellent initial uptakes into the brain (6.03 ± 0.99% ID/g) at 2 min after injection. Since there are no Aβ plaques in normal mice, the high uptake was subsequently followed by a moderate washout with 1.12% ID/g at 120 min. Compared with the fluoropegylated phenanth derivatives (3.80)<sup>14</sup>, the radioiodinated ligand [<sup>125</sup>I]5 in this study had superior brain<sub>2 min</sub>/brain<sub>120 min</sub> ratios (5.38). In addition, the blood background level during the experiment was lower than the brain uptake, which is good for reducing nonspecific binding. [<sup>125</sup>I]5 was excreted predominantly by the hepatobiliary and excretory systems, and radioactivity was observed to accumulate within the intestine at later time points (16.93% ID/g at 120 min).

A good initial uptake combined with a rapid washout from normal brain tissue are important requirements for Aβ plaque imaging agents.<sup>17</sup> The radioiodinated quinoxaline derivative [<sup>125</sup>I]5 reported here, met the first requirement but still needs some refinements to improve its washout rate.

In summary, we have developed a new type of amyloid imaging agent based on the quinoxaline pharmacophore. These derivatives displayed high affinity for Aβ<sub>1–42</sub> aggregates (*K<sub>i</sub>* values in the nM range). The radioiodinated probe [<sup>125</sup>I]5 showed specific labeling of Aβ plaques in sections of brain tissue from AD patients and transgenic mice. In addition, [<sup>125</sup>I]5 readily enters the brain and

was washed out from the normal mouse brain moderately quickly. Further refinements are under way to decrease the lipophilicity of this probe and improve its rate of washout from the brain. These quinoxaline ligands could be potentially useful for the imaging of Aβ plaques in living subjects.

## Acknowledgements

This study was supported by the Japan Society for the Promotion of Science (JSPS) through the “Funding Program for Next Generation World-Leading Researchers (NEXT Program)” initiated by the Council for Science and Technology Policy (CSTP), and a Grant-in-aid for Young Scientists (A) and Exploratory Research from the Ministry of Education, Culture, Sports, Science and Technology, Japan. This study was also supported by the China Scholarship Council (CSC).

## Supplementary data

Supplementary data associated with this article can be found, in the online version, at doi:10.1016/j.bmcl.2011.05.079.

## References and notes

- Hardy, J. A.; Higgins, G. A. *Science* **1992**, *256*, 184.
- Selkoe, D. J. *JAMA-J. Am. Med. Assoc.* **2000**, *283*, 1615.
- Hardy, J. A.; Selkoe, D. J. *Science* **2002**, *297*, 353.
- Mathis, C. A.; Wang, Y.; Holt, D. P.; Huang, G. F.; Debnath, M. L.; Klunk, W. E. *J. Med. Chem.* **2003**, *46*, 2740.
- Klunk, W. E.; Engler, H.; Nordberg, A.; Wang, Y.; Blomqvist, G.; Holt, D. P.; Bergstrom, M.; Savitcheva, I.; Huang, G. F.; Estrada, S.; Ausen, B.; Debnath, M. L.; Barletta, J.; Price, J. C.; Sandell, J.; Lopresti, B. J.; Wall, A.; Koivisto, P.; Antoni, G.; Mathis, C. A.; Langstrom, B. *Ann. Neurol.* **2004**, *55*, 306.
- Andersson, J. D.; Varnas, K.; Cselenyi, Z.; Gulyas, B.; Wensbo, D.; Finnema, S. J.; Swahn, B. M.; Svensson, S.; Nyberg, S.; Farde, L.; Halldin, C. *Synapse* **2010**, *64*, 733.
- Nyberg, S.; Jonhagen, M. E.; Cselenyi, Z.; Halldin, C.; Julin, P.; Olsson, H.; Freund-Levi, Y.; Andersson, J.; Varnas, K.; Svensson, S.; Farde, L. *Eur. J. Nucl. Med. Mol. Imaging* **2009**, *36*, 1859.
- Koole, M.; Lewis, D. M.; Buckley, C.; Nelissen, N.; Vandenbulcke, M.; Brooks, D. J.; Vandenbergh, R.; Van Laere, K. *J. Nucl. Med.* **2009**, *50*, 818.
- Rowe, C. C.; Ackerman, U.; Browne, W.; Mulligan, R.; Pike, K. L.; O'Keefe, G.; Tochon-Danguy, H.; Chan, G.; Berlangieri, S. U.; Jones, G.; Dickinson-Rowe, K. L.; Kung, H. F.; Zhang, W.; Kung, M. P.; Skovronsky, D.; Dyrks, T.; Holl, G.; Krause, S.; Friebe, M.; Lehman, L.; Lindemann, S.; Dinkelborg, L. M.; Masters, C. L.; Villemagne, V. L. *Lancet Neurol.* **2008**, *7*, 129.
- Choi, S. R.; Golding, G.; Zhuang, Z. P.; Zhang, W.; Lim, N.; Hefti, F.; Benedum, T. E.; Kilbourn, M. R.; Skovronsky, D.; Kung, H. F. *J. Nucl. Med.* **2009**, *50*, 1887.
- Kung, M. P.; Hou, C.; Zhuang, Z. P.; Zhang, B.; Skovronsky, D.; Trojanowski, J. Q.; Lee, V. M.; Kung, H. F. *Brain Res.* **2002**, *956*, 202.
- Zhuang, Z. P.; Kung, M. P.; Wilson, A.; Lee, C. W.; Plossl, K.; Hou, C.; Holtzman, D. M.; Kung, H. F. *J. Med. Chem.* **2003**, *46*, 237.
- Newberg, A. B.; Wintering, N. A.; Plossl, K.; Hochold, J.; Stabin, M. G.; Watson, M.; Skovronsky, D.; Clark, C. M.; Kung, M. P.; Kung, H. F. *J. Nucl. Med.* **2006**, *47*, 748.
- Zhang, W.; Kung, M.-P.; Hou, C.; Oya, S.; Skovronsky, D.; Manchanda, R.; Choi, S.-R.; Kung, H. *J. Nucl. Med.* **2008**, *49*, 143P.
- Hindo, S. S.; Mancino, A. M.; Braymer, J. J.; Liu, Y.; Vivekanandan, S.; Ramamoorthy, A.; Lim, M. H. *J. Am. Chem. Soc.* **2009**, *131*, 16663.
- Cai, L. S.; Innis, R. B.; Pike, V. W. *Curr. Med. Chem.* **2007**, *14*, 19.
- Kung, H. F.; Choi, S. R.; Qu, W. C.; Zhang, W.; Skovronsky, D. *J. Med. Chem.* **2010**, *53*, 933.